ISSN 1990-7931, Russian Journal of Physical Chemistry B, 2017, Vol. 11, No. 7, pp. 1061–1069. © Pleiades Publishing, Ltd., 2017.
Original Russian Text © M.Yu. Tsvetkov, V.I. Yusupov, P.S. Timashev, K.M. Golant, N.V. Minaev, S.I. Tsypina, V.N. Bagratashvili, 2016, published in Sverkhkriticheskie Flyuidy. Teoriya i Praktika, 2016, Vol. 11, No. 2, pp. 14–27.

On the Role of Supercritical Water in Laser-Induced Backside Wet Etching of Glass

M. Yu. Tsvetkov[a], V. I. Yusupov[a, *], P. S. Timashev[a], K. M. Golant[b], N. V. Minaev[a], S. I. Tsypina[a], and V. N. Bagratashvili[a, c]

[a] *Institute of Photonic Technology Federal Center Crystallography and Photonics, Russian Academy of Sciences, Troitsk, Moscow, 108840 Russia*

[b] *Kotel'nikov Institute of Radio Engineering and Electronics, Russian Academy of Sciences, Moscow, 125009 Russia*

[c] *Department of Chemistry, Moscow State University, Moscow, 119991 Russia*

**e-mail: iouss@yandex.ru*

Received April 3, 2016

Abstract—The features and mechanisms of microcrater formation in optical silicate glass by laser-induced backside wet etching (LIBWE) are determined in a wide range of energy densities (Φ) from 4 to 10^3 J/cm^2 for laser pulses of 5 ns length and 1 kHz repetition rate. The existence of two different mechanisms of laser-induced microcrater formation is revealed: (i) chemical etching in supercritical water (SCW), and (ii) cavitation. At $\Phi > 10^2$ J/cm^2 irregular craters of 1–20 μm in depth with rough walls and distinct cracks around microcrater are formed testifying that in such mode ("hard") laser induced cavitation plays a dominant role in glass removal. At $\Phi <$ J/cm^2 neat glass craters with smooth walls are formed, their size and shape are easily reproducible, cracks are not formed, and the processing area is limited to the laser spot area. In this mode ("soft mode with active cavitation"), a microcirculation of water is stimulated by cavitation without causing undesirable shock breakage. The latter is achieved thanks to the fast removal of glass etching products by microcirculation, and the inflow of "fresh" etchant (SCW) to the glass surface in the vicinity of the formed microcraters. Such mode is optimal for highly controlled laser microstructuring of glass and other optically transparent materials.

Keywords: laser-induced liquid etching, supercritical water, cavitation, microstructuring

DOI: 10.1134/S1990793117070181

INTRODUCTION

One of the effective approaches to the formation of microstructures on the surface of optically transparent materials is based on pulsed laser-induced backside wet etching (LIBWE) [1–4]. In the Russian-speaking literature, there is no equivalent well-established term, and it can be named as laser liquid etching. The LIBWE method is based on the focusing of pulsed-periodic laser radiation on the back surface of an optically transparent sample bordering on a liquid that strongly absorbs laser radiation. Absorption of a focused laser pulse by the liquid leads to a rapid increase in temperature at the boundary of the sample, which is accompanied by the removal of a part of its material. Using pulsed-periodic laser radiation and a suitable highly absorbing liquid solution, it is possible to form very accurately various microstructures on the surface of a transparent sample by moving the point of focus along a given trajectory [5] or by creating interference patterns [6].

The LIBWE process can provide a low roughness of the inner surface of the resulting crater (the mean square deviation <10 nm) [7], the possibility of obtaining channels in an optical material with a large ratio of their depth to the width (up to ~30 [8, 9]). Therefore, this method is very promising for the creation of new elements of microelectronics, microoptics [7, 10, 11], and microfluids [12].

As for the mechanism of pulsed laser etching of the back surface of a transparent sample in a liquid, it has been poorly studied. Among the techniques under consideration, we especially note cavitation destruction and/or material removal associated with the formation and stripping of bubbles (accompanied by high impulse pressures) [13] and chemical etching in supercritical water formed using the fast-pulsed heating of the aqueous solution [14]. These contributions to the LIBWE process can largely depend on the temporal and amplitude parameters of the sudden temperature and pressure changes that occur in the region of the laser pulse action. By changing these parameters, for example, by changing the energy and duration of the laser pulse or the surface tension in the absorbing liquid (on which the effect of cavitation is substantially dependent [15]), the relative contribution of each can

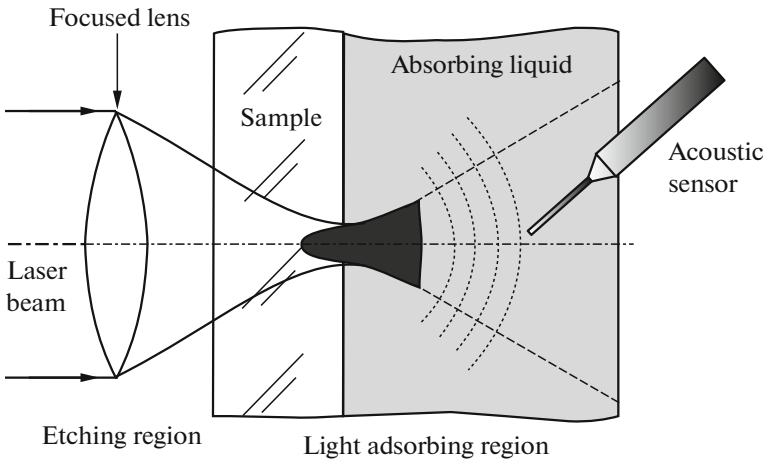

Fig. 1. Scheme of laser etching of the crater in the sample of borosilicate glass with focused laser radiation.

be selectively varied. Each individual contribution be assessed by visual observation of the impressions using optical, electron, or atomic force microscopy. A sensitive and very convenient method for studying laser-induced hydrodynamic processes, in particular, the cavitation arising during the LIBWE process, is the optoacoustic method [14, 16] based on the measurement of acoustic fields near the field of laser action by means of needle hydrophones. It allows us to determine the boundary of the transition from "soft" (well-controlled) to "hard" (impact, poorly controlled) pulsed laser action on a transparent material [14, 16], which is important for implementing the technology of a well-controlled laser microstructuring based on the considered LIBWE method.

In this paper, we show that both these laser-induced processes (cavitation and formation of supercritical water (SCW)) play an important role in the LIBWE process. Moreover, conditions are found under which cavitation, without causing undesirable destruction of glass, makes it possible to significantly accelerate the etching process of the SCW glass. This is ensured by the rapid removal of glass etching products by cavitation-generated microcirculations and the inflow of a "fresh" etching agent into the glass surface in the region of the crater to be formed.

EXPERIMENTAL

As samples of a transparent material for the study of the LIBWE process, standard microscopic glasses made of silicate glass with dimensions of 75 × 25 × 1 mm were used; the approximate composition is the following: SiO_2, 73%; Na_2O, 14%; CaO, 7%; MgO, 4%; and Al_2O_3, 2%. The sample to be laser etched was installed as the front wall of a demountable cuvette which was filled with an absorbing liquid (Fig. 1).

The effect on the back surface of the optically transparent sample bordering on the absorbing liquid was carried out by the second harmonic of the solid-state laser TECH-527 Basic (Laser-compact, Russia) at a wavelength of 527 nm with a laser pulse duration of ~5 ns, a maximum pulse energy of 250 μJ, and with a pulse frequency repetition of 1 kHz. To focus the radiation on the back surface, a Thorlabs LMH-10X-532 10× lens with a numerical aperture NA = 0.25 was used (Fig. 1).

As an absorbing liquid, an aqueous solution of food coloring Amaranth (Sigma-Aldrich) [17] was used in the experiments. The absorption spectra of the dye solutions were determined using a Shimadzu UV-3600 spectrophotometer. The absorption coefficient of this dye at a wavelength of 527 nm using a saturated dye solution (0.1 mol/L) was 2×10^3 cm^{-1}, which provided absorption of ~90% of the laser radiation in the 10 μm layer of the absorbing liquid (the absorption region is conventionally shown in Fig. 1). In experiments, to reduce the surface tension coefficient, polyethylene glycol (PEG) was added to the dye solution at a concentration of 20 vol %. At this concentration, the coefficient of surface tension decreases by approximately 30%, and with a further increase in the concentration of polyethylene glycol, there is practically no decrease in the coefficient.

The cuvette with the sample was placed on a Standa 8MT167-100 software-controlled three-coordinated shift with a positioning accuracy exceeding 0.5 μm. After the formation of the regular crater in the sample of silicate glass (exposure time 10 s), the cuvette was moved with the controlled shift to a predetermined distance, and the laser was turned on again to produce the next crater.

The geometry, shape, and characteristics of the surface of the craters formed in the samples were studied using optical microscopy (an HRM-300 Huvitz optical microscope), scanning electron microscopy (SEM, a Phenom ProX microscope), and atomic force microscopy (AFM "INTEGRA-Terma", NT-MDT).

Table 1. Characteristics of the process of crater formation and dominant mechanisms under different LIBWE modes

No.	Processing mode	Process parameters	Characteristics of the formation process and laser crater parameters	Dominant mechanism of material removal
1	Hard mode	$\Phi > 10^2$ J/cm^2	High wall roughness of the crater; formation of cracks outside the crater; high rate of material removal; low repeatability of the shape of the crater; large amplitude of the shock wave	Impact (cavitational) removal of the material
2	Soft mode with active cavitation	$\Phi < 50$ J/cm^2	Low roughness of crater walls; no cracks outside the crater; high repeatability of the crater shape; presence of the "edge" around the crater; high etching rate; moderate amplitude of the shock wave	Glass etching in SCW; cavitation removal of laser etching products in SCW; acceleration of the inflow of SCW to the boundary with the material
3	Soft mode with suppressed cavitation	$\Phi < 50$ J/cm^2; with addition of PEG	Smooth crater walls; no cracks outside the crater; high repeatability of the shape of the crater; absence of the "edge" around the crater; small amplitude of the shock wave	Etching of glass in SCW; slow removal of laser etching products in SCW

The study of the hydrodynamic processes caused by fast laser heating, arising in the process of cavity-free cavitation, was carried out using the optoacoustic method. This required recording the acoustic signals accompanying the fast laser heating of the aqueous solution using a needle hydrophone with a 1-mm diameter of the sensor area with a flat (±4 dB) spectral characteristic in the range of 200 kHz–15 MHz and a sensitivity of 850 nV/Pa. The sensory end of the needle hydrophone was located in the absorbing fluid near the optic axis of the laser beam at a distance of 7 mm from the region of the laser action (Fig. 1). The signals from the hydrophone passed through a Precision Acoustics preamplifier were recorded with a GW Instek GDS 72304 memory oscilloscope with a bandwidth of 300 MHz. The value of the pressure was recalculated to a distance of 3 μm from the surface of the sample assuming a spherical divergence of the wave from the laser action region.

RESULTS AND DISCUSSION

The formation of laser craters in optical plates made of silicate glass by the LIBWE method was performed at a laser pulse energy in the range of 0.5–130 μJ. The diameter of the laser spot focused on the back surface of the transparent sample was 3.4 ± 0.4 μm, i.e., the range of energy densities (Φ) of the laser pulse used was 4–10^3 J/cm^2. Experiments have shown that from the point of view of the nature of the laser imprint in the sample and the character of the optoacoustic response, three different modes of action clearly appear (Table 1, Figs. 2 and 3): (1) "hard" mode (with strong cavitation) occurring at $\Phi > 10^2$ J/cm^2; (2) "soft mode with active cavitation" at $\Phi < 50$ J/cm^2; (3) "soft mode with suppressed cavitation" at $\Phi < 50$ J/cm^2, and the addition of PEG to the aqueous solution, significantly reducing the surface tension of the solution.

Figure 2 shows the SEM images of the craters obtained in the sample corresponding to each of the three listed modes ("hard", "soft with active cavitation", and "soft with suppressed cavitation").

It can be seen that in the hard mode, a crater with uneven edges and wide expanding cracks is formed (Fig. 2a). When reducing the amplitudes of the pulsed pressure associated with cavitation by more than an order of magnitude and passing to the soft mode with active cavitation (Fig. 2b), a regular-shaped crater with a diameter at the level of the sample surface ~4 μm is formed on the surface of silicate glass. The reduction of the cavitation by adding a surfactant to the water solution when passing to the soft mode with suppressed cavitation (Fig. 2c) leads to a decrease in the etching rate, and the crater diameter decreases to ~2.5 μm.

Figure 3 shows fragments of acoustic signals registered during laser etching of a sample of silicate glass in three modes: hard, soft with active cavitation, and soft with suppressed cavitation (these signals correspond to the same cases of the LIBWE modes, SEM images for which are presented in Fig. 2).

When decreasing the energy in the laser pulse and passing from the hard mode (Fig. 3a) to the soft mode with active cavitation (Fig. 3b), the amplitudes of acoustic pulses decrease by a factor of 5–10, which indicates a significant decrease in the energy of cavitation. In the case when PEG is added to the aqueous solution of the dye, the amplitudes of the recorded acoustic pulses decrease by approximately an order of

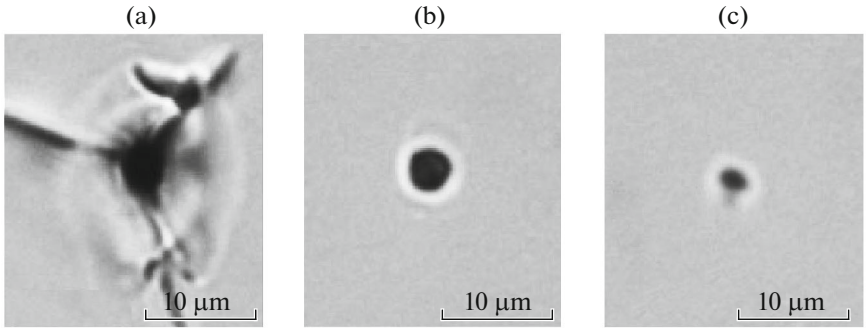

Fig. 2. SEM images of craters in silicate glass obtained in the process of laser etching for three modes: (a) hard mode with strong cavitation ($\Phi = 200$ J/cm^2); (b) soft with active cavitation ($\Phi = 35$ J/cm^2);(c) soft with suppressed cavitation ($\Phi = 35$ J/cm^2, with the addition of PEG).

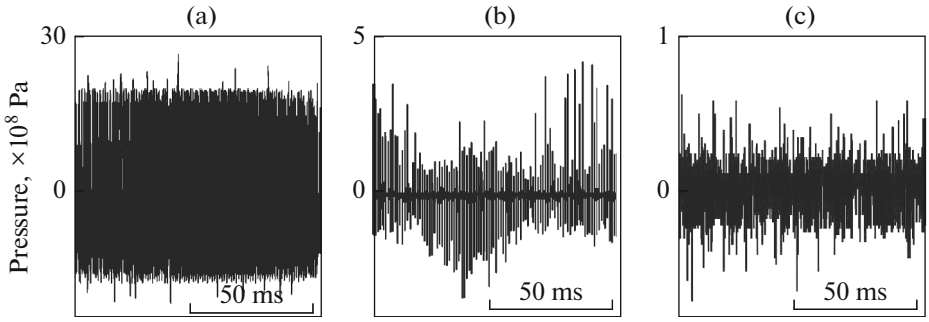

Fig. 3. Fragments of acoustic signals obtained in the process of laser etching for three modes: (a) hard with strong cavitation ($\Phi = 200$ J/cm^2); (b) soft with active cavitation ($\Phi = 35$ J/cm^2); (c) soft with suppressed cavitation ($\Phi = 35$ J/cm^2, with the addition of PEG).

magnitude (Fig. 3c), which indicates a significant suppression of cavitation.

Hard Mode for Removing Material

At a laser radiation energy density of $\Phi > 10^2$ J/cm^2, irregular laser craters with a depth of 1–20 μm with strongly broken walls are formed in glass with distinct cracks around them. In this mode (which we called hard [14]), with an increasing number of laser pulses the depth of the laser crater and its width increase (exceeding the region of the laser spot). No cracks appear at first laser pulses, but they begin to appear distinctly after a certain laser exposure, which is apparently due to the accumulation of internal defects and their manifestation upon further irradiation. This indicates the impact nature of the glass treatment in this hard mode (Fig. 3a) demonstrating the formation of intense shock waves, which obviously cause the impact destruction of glass when the impulse pressures associated with cavitation (caused by a fast laser heating of water [18]) exceed the strength of the transparent material. This hard LIBWE mode is characterized by low repeatability and bad controllability of the glass treatment, and therefore it is practically not suitable for the formation of well-controlled microstructures in glass.

Soft Etching Modes

With a decrease in the energy density of the laser pulse to 50 J/cm^2 (and lower), the formation of the crater becomes more controllable, the depth of the crater increases with the number of pulses, and no cracks are formed around the crater. In addition, the roughness and unevenness of the wall surface of the crater are significantly reduced. The diameter of the crater in this case is approximately equal or slightly smaller than the diameter of the laser spot. An important feature of this mode is the formation of a distinct "border" around the laser crater (Fig. 4), which we associate with the ejection of etching products from the crater by liquid streams that result from cavitation and cause no impact failure of glass. That is why we call this mode the soft mode with active cavitation.

Adding a certain amount of PEG to the dye solution, which reduces the surface tension of the solution by 30%, causes a significant decrease in the etching rate of glass and suppression of the amplitude of the

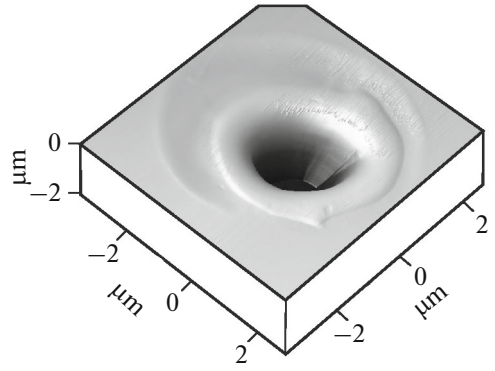

Fig. 4. AFM image of the crater formed in the soft mode with active cavitation.

optoacoustic signal associated with cavitation (see Fig. 3) with the same value of Φ.

The differences in the shape of the crater in silicate glass during laser etching in the soft mode with active cavitation and soft mode with suppressed cavitation are clear more distinctly from a comparison of crater profiles obtained using AFM (Fig. 5). The crater obtained in the soft mode with active cavitation (Fig. 5d) has a V-shaped profile (inverted cone), a depth of ~600 nm, and a diameter at the sample surface level of ~4.5 μm. Passing to the soft mode with suppressed cavitation (Fig. 5b) results in a significant decrease in the etching rate. In this case, the crater has the shape of an inverted truncated cone, its diameter at the surface level slightly decreased to ~3.8 μm, and the depth decreased almost 6 times to ~110 nm.

Another significant difference between the craters when passing from the laser etching mode with the active cavitation to the suppressed cavitation mode is a substantial decrease in the small-scale fluctuations in the depths of the crater profiles (Fig. 5b), i.e., to a decrease in the roughness of their inner surface.

To clarify the role of SCW in the LIBWE mechanism, laser-induced etching of the core and a shell of the end section of a preform of a multimode optical fiber with a quartz shell and a core with a GeO_2 content of 10% were compared. To make this, a ~1 mm thick disk was cut from the preform, which was placed inside the cuvette with an absorbing liquid on its front

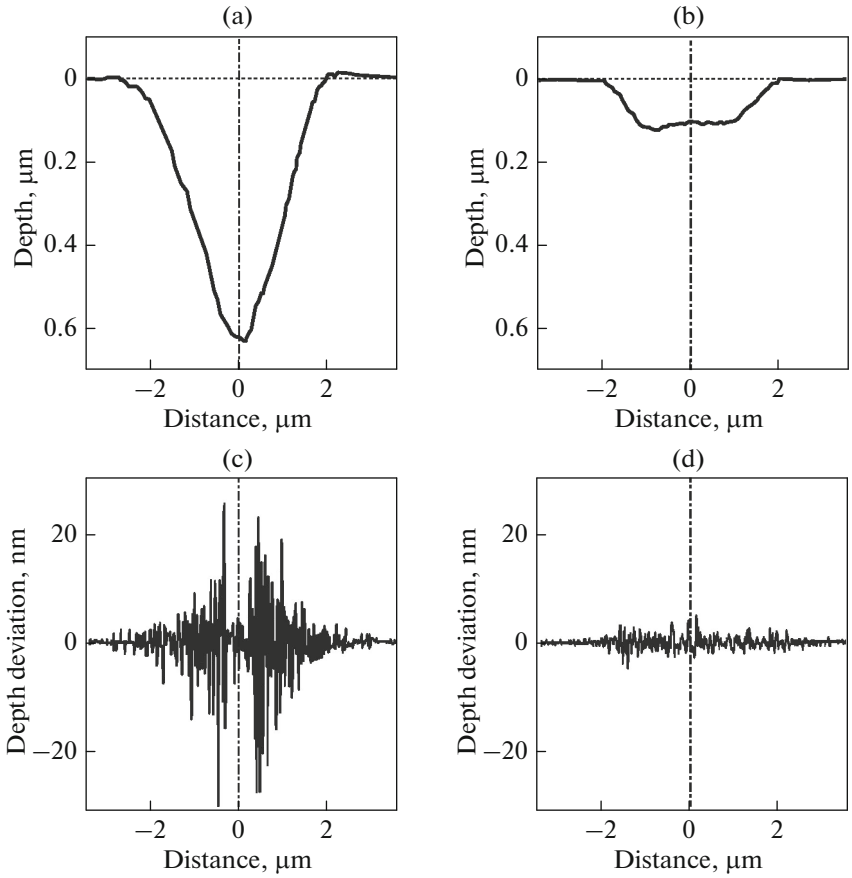

Fig. 5. AFM profiles (top) and small-scale fluctuations in the depths of profiles of the corresponding craters (bottom) obtained in silicate glass during laser etching, for (a) soft mode with active cavitation and (b) soft mode with suppressed cavitation; in both cases, $\Phi = 35$ J/cm^2.

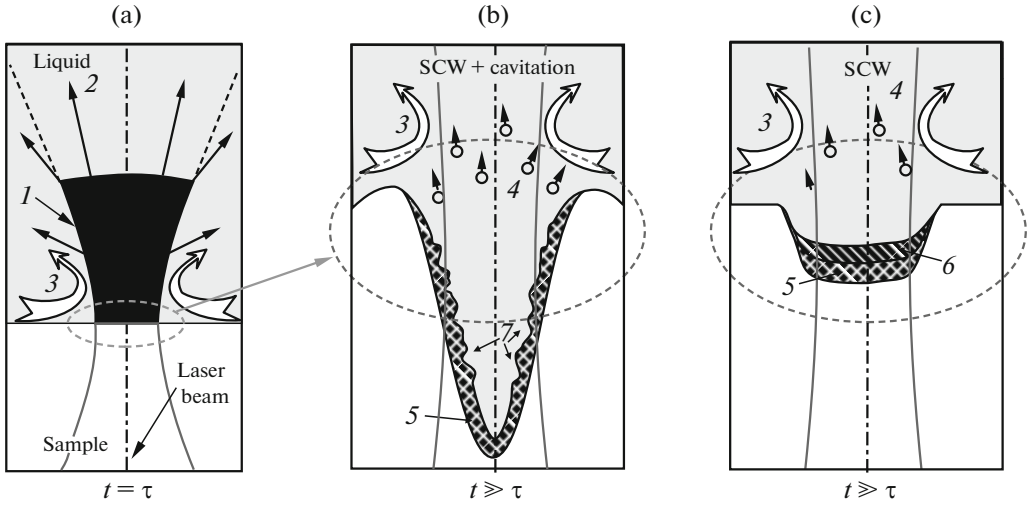

Fig. 6. Diagram explaining the mechanism of the action of the LIBWE for soft modes at different moments of time (t): (a) in the moment when the first laser pulse ends ($t = \tau$); (b) for $t \gg \tau$ for soft mode with active cavitation; (c) for $t \gg \tau$ for soft mode with suppressed cavitation; (*1*) the area in which the laser energy is absorbed; (*2*) directions of expansion of the region with high temperature and pressure; (*3*) streams in a liquid; (*4*) the particles of the transparent sample etched with SCW carried by the laser-induced flow; (*5*) softened area of the transparent sample; (*6*) a thin layer with the substance of a transparent sample etched with SCW; (*7*) a part of the softened layer (*5*) destroyed by cavitation.

wall. It was shown [19] that when etched in supercritical water the etching rate of the core of such a fiber is much higher than the etching rate of its shell. This is due to the fact that, due to the larger ionic radius of Ge compared with Si, the glass network becomes more strained, which can lead to the formation of microcracks. In addition, the introduction of germanium initiates the formation of high ($>10^{20}$ cm^{-3}) concentrations of point defects of the type of oxygen-deficient centers in the glass network [20]. Our experiments showed that in the soft mode with suppressed cavitation, the rate of LIBWE of the germanosilicate core of the preform is several times higher than the etching rate of the quartz shell, which was observed in [19].

Modes of Laser Etching

The table summarizes the main observations for all three modes of material removal in the LIBWE process.

Let us consider in more detail the possible ways pulsed laser etching of glass works in two practically important and most interesting modes, the soft mode with active cavitation and the soft mode with suppressed cavitation.

We assume that the differences in shape, size, and quality of the surface of the craters formed in silicate glass as described above when passing from one mode to another are explained by the different contribution of the two main processes of material removal caused by strong pulsed laser water heating: (1) chemical etching with supercritical water; and (2) cavitation failure.

The main processes that take place when a focused pulsed laser radiation is exposed to the back surface of an optically transparent sample bordering the absorbing liquid are schematically shown in Fig. 6, where two hyperbolas indicate the region of action of laser pulsed radiation focused on the transparent image/liquid boundary. For two "soft" modes, the laser etching mechanism is due to: (i) etching with SCW, cavitation removal of the material etched with SCW (*4*), and cavitation destruction of the softened layer (*5*) (Fig. 6b); and (ii) only by etching with SCW (Fig. 6c).

Initially, a small subsurface volume of liquid (*1*) is heated (see Fig. 6a) because of the absorption of laser radiation. The volume of this region is determined by the geometric parameters of the focusing of laser radiation (a hyperbola in Fig. 6a) and by the distance at which about 90% of the laser energy is absorbed, approximately equal to $2\alpha^{-1} = 10$ μm ($\alpha = 2 \times 10^3$ cm^{-1} is the absorption coefficient). In our case, almost all the laser energy is absorbed in a volume of ~150 μm^3. The absorption of the energy of a short laser pulse (duration τ) in such a small volume of liquid leads to the fact that at the end ($t = \tau$) the liquid will be heated up to the temperature [1]

$$T = T_0 + \frac{\Phi\left(1 - \exp(-\alpha d_{\mathrm{T}}^{\mathrm{L}})\right)}{\rho^{\mathrm{G}} C_p^{\mathrm{G}} d_{\mathrm{T}}^{\mathrm{G}} + \rho^{\mathrm{L}} C_p^{\mathrm{L}} d_{\mathrm{T}}^{\mathrm{L}}}, \qquad (1)$$

where $T_0 \approx 300$ K is the initial temperature; $\Phi = E/S$ is the density of the laser radiation energy; E is the energy of the laser pulse; S is the laser area on the surface of the sample bordering with the absorbing liquid;

ρ is the density; C_p is the specific heat; $d_T = \sqrt{4D_T\tau}$ is the depth of thermal heating; D_T is the coefficient of thermal conductivity; and τ is the length of the laser pulse (the upper indices L and G refer to the liquid and glass, respectively). Substituting the table values $\rho^L = 1000$ kg/m^3, $\rho^G = 2500$ kg/m^3, $C_P^L = 4200$ J/(kg K), $C_P^G = 700$ J/(kg K), $D_T^L = 1.4 \times 10^{-7}$ m^2/s, $D_T^G = 3.4 \times 10^{-7}$ m^2/s, and $\tau = 5 \times 10^9$ s, for the soft mode with an energy of laser pulses of $E = 4$ μJ we obtain $T \approx 1.7 \times 10^4$ K. Thus, the absorption of the laser pulse heats the volume of liquid (*1* in Fig. 6a) to a temperature of $T \gg T_c$, where $T_c \approx 647$ K is the critical temperature of water.

In the case of the predominance of thermal diffusion, the characteristic lifetime of this heated region with supercritical water can be estimated from the time of thermal relaxation:

$$\tau_T = \frac{L^2}{D_T^L} \approx 200\ \mu s, \quad (2)$$

where $L \approx 5$ μm is the characteristic size of the heated region. However, at high temperatures, phase transitions must be considered. As shown by theoretical calculations and experimental studies, explosive boiling of liquid takes place at a temperature as low as (0.9–1.0)$T_c \approx 590$–650 K with the formation of a bubble in the region of laser action expanding at a high velocity [21]. Rapid expansion of the bubble leads to its equally rapid cooling and causes intensive mixing of the liquid. It is well known [22] that a bubble reaching its maximum radius R_{max} cavitates and collapses. When the bubble contracts to very small size (<1 μm), its potential energy is converted into the kinetic energy of the high-speed (up to 10^3 m/s) stream and into the acoustic energy of the shock wave expanding in all directions [23]. When the bubble collapses near the solid wall of the back surface of the sample, this stream is directed toward the wall. It is known that these streams can destroy the surface of quartz glass forming micron-sized holes and other defects [18].

In our case, the intensity of these laser-induced hydrodynamic processes was recorded using acoustic measurements. As it is seen from Fig. 3, when passing from the soft mode with active cavitation to soft mode with suppressed cavitation, the amplitude of the acoustic pulses decreased by approximately an order of magnitude, which confirms the suppression of cavitation with the addition of PEG to the aqueous dye solution. At the same time, the pressure amplitudes in the soft mode with active cavitation fell in the range of 100–400 MPa (Fig. 6b), and in the soft mode with suppressed cavitation (Fig. 3c) they varied within the range of 25–60 MPa, i.e., in both cases it exceeded the value of the critical pressure for water $P_c = 22.1$ MPa.

Thus, it is shown that under the laser action both the temperature and pressure of the near-surface liquid layer (*1* in Fig. 6a) are increased to values exceeding the corresponding critical values for water when the laser pulse is applied. This means that there is water in the supercritical state in the crater formation area. Therefore, the differences in shape, size, and quality of the surfaces of craters formed in silicate glass when passing from the soft mode with active cavitation to soft mode with suppressed cavitation can be explained by the different contribution of cavitation fracture and chemical etching by supercritical water.

In the soft mode with active cavitation, an important role is played by the cavitation removal of the substance, which leads to the formation of a crater in the form of an inverted cone. This leads to an increased level of roughness of the surface of the crater (Fig. 5a) and to the appearance of a crater edge projecting over the surface (see Figs. 4, 5a, 6b), which we directly connect with the partial removal (extrusion) of the material heated to high temperatures by high-pressure pulses [14] and precipitation of the sample material dissolved in supercritical water [24]. Note that in [24], when etching canals in borosilicate glass placed in a reactor with supercritical water, similar regions projecting over the glass surface with a thickness of up to 7 μm were observed along the channels. In this case, the precipitation of glass dissolved by supercritical water occurred only if the SCW density in the reactor exceeded 0.5 g/cm^3.

We emphasize that in the very center of the crater (Fig. 5a below) a smoother region with a transverse size of ~600 nm clearly stands out. We explain this by the fact that supercritical water down the crater is delayed for a longer time due to a decrease in the mixing rate associated with the geometry.

In the "soft mode with suppressed cavitation", there is no microcirculation and removal of the substance. This leads to a decrease in the etching rate and the formation of craters with smooth surfaces and a practically flat bottom (Fig. 4b). The suppression of cavitation also leads to the absence of a crater edge projecting over the surface, which is characteristic of the mode with developed cavitation. Strengthening the role of supercritical water in the etching of the material is because it is retained in the crater for a longer time because of a decrease in the flow velocity (streams 3 in Fig. 6c). Because the area with supercritical water is mixed, the walls of the crater are etched in all directions at approximately the same rate, which leads to the formation of an almost flattened bottom.

We studied the influence of the process on the LIBWE mechanism in detail. The region with increased pressure and temperature due to the presence of a boundary with a solid will expand mainly in the direction of the free liquid, as it occurs when generating vapor-gas bubbles by a heated turn of the laser fiber [25]. The rate of expansion of the heated region can be assessed using the relation [26]:

$$V = \sqrt{\frac{2}{3}\frac{\Delta p}{\rho^{L}}}, \quad (3)$$

where Δp is the abrupt pressure change determined from acoustic measurements. Since for the soft mode with active cavitation (Fig. 3b) $\Delta p \sim 100$–400 MPa, and for the soft mode with suppressed cavitation (Fig. 3c) $\Delta p \sim 25$–60 MPa, the expansion rates will be 260–520 and 130–200 m/s, respectively. We note that temperature at the boundary of the surface of the sample and the absorbing liquid was calculated above by Eq. (1) [1] without taking into account the absorption at the boundary [13], which gradually increases in the multipulse laser etching mode due to the formation of an adsorbed layer of products of photo and thermal destruction of the dye on the surface. These products (mainly nano- and microparticles of carbon) will accumulate near the region of the laser action also due to the Marangoni convection and capture of nanoparticles from the liquid volume by laser-induced bubbles [23]. These bubbles could have been formed by gases dissolved in water and by gaseous products (H_2, CO, CO_2, CH_4) of the decomposition of the dye and PEG and their oxidation by water.

The results of our experiment (see above) show that the SCW generated during fast laser heating plays a crucial role in the LIBWE mechanism demonstrating a much higher etching rate of the germanosilicate core of the preform than its quartz shell, which is completely analogous to the results on the etching of similar materials in SCW obtained in [19].

CONCLUSIONS

The experiments on the formation of craters in an optical plate made of silicate glass with rapid heating of water at the water/glass boundary by high-power laser pulses allowed us to determine three laser processing modes determined both by the energy density of the laser radiation Φ and the surface tension of the solution.

(1) For sufficiently large Φ (more than 10^2 J/cm^2), laser craters with a depth of 1–20 μm with rough walls are formed with distinct cracks around them indicating the impact character of the action on glass in this hard mode. The nature of the optoacoustic signals recorded directly indicates the occurrence of intense shock waves, which obviously lead to the destruction of glass, since the impulse pressures associated with cavitation (caused by rapid laser heating of water) exceed the ultimate strength of the transparent material. It is clear that this hard exposure mode is not suitable for creating well-controlled microstructures in glass.

(2) At smaller values of Φ (below 50 J/cm^2), neat laser craters with smooth walls are formed in glass; the dimensions and shape of the craters are reproducible, cracks are not formed, and the processing area is limited to the zone of the laser spot. It was determined that in these cases, under laser action both the temperature and the pressure of the near-surface liquid layer are increased to values higher than the corresponding critical values for water. Acoustic measurements show that shock waves are also formed in this case, but they are of a significantly (by an order of magnitude) lower intensity. They do not cause damage of glass outside the irradiation zone. This etching mode (the soft mode with active cavitation) is quite suitable for creating well-controlled microstructures in glass.

(3) When the surface tension of the aqueous solution is lowered (by adding PEG to it), the etching rate of glass decreases several times, the walls of the crater become smoother, its bottom is almost flat, and the acoustic measurements demonstrate a significant (almost an order of magnitude) suppression of the cavitation signal. We call this etching mode the soft mode with suppressed cavitation.

Thus, supercritical water and cavitation play an important role in the mechanism of well-controlled laser-induced backside wet etching based on pulsed laser heating of a highly absorbing liquid near the back surface of a transparent sample. The conditions of LIBWE (soft mode with active cavitation) are found in which cavitation without causing undesirable destruction of glass allows the glass etching process to be accelerated considerably. This is ensured by the rapid removal of etched products by means of the cavitation-induced microcirculation and the inflow of a "fresh" etching agent (SCW) to the glass surface in the region of the microcrater formed.

ACKNOWLEDGMENTS

This work was supported by the Russian Science Foundation, project no. 14-33-00017 (regarding the role of supercritical water in the laser etching process) and the Government of the Russian Federation for State Support of scientific research carried out under the supervision of leading scientists, contract 14.B25.31.0019 (in the part of studying the processes of laser micro- and nanostructuring of glass).

REFERENCES

1. J. Wang, H. Niino, and A. Yabe, Appl. Phys. A **68**, 111 (1999).
2. J. Wang, H. Niino, and A. Yabe, Appl. Phys. A **69** (Suppl.), S271 (1999).
3. H. Niino, Y. Yasui, X. Ding, A. Narazaki, T. Sato, Y. Kawaguchi, and A. Yabe, J. Photochem. Potobiol. A: Chem. **158**, 179 (2003).
4. K. Zimmer, M. Ehrhardt, and R. Böhme, in *Laser Ablation in Liquids: Principles and Applications in the Preparation of Nanomaterials,* Ed. by G. Yang (Pan Stanford, Singapore, 2012).
5. J.-Y. Cheng, M.-H. Yen, and T.-H. J. Young, Micromech. Microeng. **16**, 2420 (2006).

6. C. Vass, K. Osvay, T. Véso, B. Hopp, and Z. Bor, Appl. Phys. A **93**, 69 (2008).
7. K. Zimmer and R. Böhme, Opt. Lasers Eng. **43**, 1349 (2005).
8. Y. Kawaguchi, H. Niino, T. Sato, A. Narazaki, and R. Kurosaki, J. Phys.: Conf. Ser. **59**, 380 (2007).
9. H. Niino, Y. Kawaguchi, T. Sato, A. Narazaki, and R. Kurosaki, Appl. Surf. Sci. **253**, 8287 (2007).
10. M. Konstantaki, P. Childs, M. Sozzi, and S. Pissadakis, Laser Photon. Rev. **7**, 439 (2013).
11. G. Kopitkovas, T. Lippert, J. Venturini, C. David, and A. Wokaun, J. Phys.: Conf. Ser. **59**, 526 (2007).
12. J.-Y. Cheng, M.-H. Yen, C.-W. Wei, Y.-C. Chuang, and T.-H. Young, J. Micromech. Microeng. **15**, 1147 (2005).
13. K. Zimmer, R. Böhme, M. Ehrhardt, and B. Rauschenbach, Appl. Phys. A **101**, 405 (2010).
14. M. Yu. Tsvetkov, V. I. Yusupov, N. V. Minaev, A. A. Akovantseva, P. S. Timashev, K. M. Golant, B. N. Chichkov, and V. N. Bagratashvili, Opt. Laser Technol. (in press).
15. M. G. Sirotyuk, in *Acoustic Cavitation,* Ed. by V. A. Akulichev and L. R. Gavrilov (Nauka, Moscow, 2008) [in Russian].
16. V. I. Yusupov, V. M. Chudnovskii, and V. N. Bagratashvili, Laser Phys. **24**, 015601 (2014).
17. M. Snehalatha, C. Ravikumar, N. Sekar, V. S. Jayakumar, and I. H. Joe, J. Raman Spectrosc. **39**, 928 (2008).
18. V. I. Yusupov, V. M. Chudnovskii, and V. N. Bagratashvili, Laser Phys. **21**, 1230 (2011).
19. V. N. Bagratashvili, A. N. Konovalov, A. A. Novitskiy, M. Poliakoff, and S. I. Tsypina, Russ. J. Phys. Chem. B **3**, 1154 (2009).
20. Yu. S. Zavorotny, A. O. Rybaltovskii, P. V. Chernov, V. N. Bagratashvili, V. K. Popov, S. I. Tsypina, and L. Dong, Glass Phys. Chem. **23**, 444 (1997).
21. V. P. Skripov, E. N. Sinitsyn, P. A. Pavlov, et al., *Thermal and Physical Properties of Liquids in a Metastable State* (Atomizdat, Moscow, 1980) [in Russian].
22. A. Vogel, W. Lauterborn, and R. Timm, J. Fluid Mech. **206**, 299 (1989).
23. V. I. Yusupov, S. I. Tsypina, and V. N. Bagratashvili, Laser Phys. Lett. **11**, 116001 (2014).
24. P. Karásek, J. Grym, M. Roth, J. Planeta, and F. Foret, Lab on a Chip **15**, 311 (2015).
25. V. I. Yusupov, V. M. Chudnovskii, and V. N. Bagratashvili, Laser Phys. **20**, 1641 (2010).
26. A. Prosperetti and M. S. Plesset, J. Fluid Mech. **85**, 349 (1978).

Translated by V. Avdeeva